Discrete Chiral Single-Crystal Microtubes Assembled with Honeycomb Coordination Networks Showing Structural Diversity and Borromean Topology in One Single Crystal

Xue-Li Zhang, Cui-Ping Guo, Qing-Yuan Yang, Tong-Bu Lu, Ye-Xiang Tong, and Cheng-Yong Su*

MOE Laboratory of Bioinorganic and Synthetic Chemistry/ State Key Laboratory of Optoelectronic Materials and Technologies, School of Chemistry and Chemical Engineering, Sun Yat-Sen University, Guangzhou 510275, P. R. China

Received July 4, 2007
Revised Manuscript Received July 25, 2007

In spite of the abundance of tubular entities in nature,[1] synthetic tubular architectures have not drawn so much attention until the discovery of carbon nanotubes.[2] Since then, there has been immense interest in the design and construction of artificial nano/microscale hollow materials due to a wide perspective in the fields of nano- and biotechnology, chemical sensors and reactors, and drug deliver or channel systems.[3] Significant progresses have been made individually in studies of organic[4] and inorganic[3] tubular structures, advancing to a goal to fabricate tubular materials with sufficiently high crystal quality at all length scales from macroscopic down to the molecular level.[5] Nevertheless, investigations on the nanocrystals based on the metal-organic coordination assemblies remain in their infancy.[6]

It is well-known that one of the most important goals pursued in the fields of coordination crystal engineering and molecular architecture is to create channels or cavities.[7] Such porosity, in principle, is related to the metal-organic framework in the crystal lattice and therefore attributable to lattice pores. By contrast, discrete crystal tubes provide physically independent channels on the basis of individual crystals, which can be regarded as crystal pores. This means that the lattice pore relies on molecules arrangement in the crystal lattice, usually limited to nanoscale coordination space.[8] However, crystal pores can vary in multiple scales depending on crystal size and morphology.[5] Although crystal pores are normally pursued in nanomaterials, whereas crystal engineering pays more attention to lattice pores, fabrication of crystal pores by making use of a crystal engineering strategy may be a prospective route. One example is the amplification of lattice pores into discrete crystal pores with the organic peptide nanotubes.[9] As a bridge to span these two important fields, growth of crystal tubes from coordination polymers may represent another perspective in synthetic tubular architectures, which takes advantage of easy incorporation of structural diversity and physical property inherent in metal-organic hybrid materials.

We have previously assembled coordination frameworks containing lattice pores of single-wall tubular channels, fullerene-like cages, or nanotubes.[10] In this paper, we report spontaneous resolution of enantiomeric pure single-crystal microtubes containing discrete crystal pores and showing intriguing Borromean topological intercalation of two structurally diversified (6,3) networks assembled via metal−ligand interactions.

A semirigid tripodal ligand, 1,3,5-tris(4-((2-ethyl-benzimidazol-1-yl)methyl)phenyl)benzene (**L** as shown in Scheme 1) featuring a large basal plane and three free-rotating pendants was synthesized (see the Supporting Information). Reaction of the ligand with $AgCF_3SO_3$ afforded hexagonal tubular crystals with sufficiently high crystallinity suitable for the single-crystal X-ray diffraction measurements.[11] The crystal analysis unambiguously revealed the chiral space group *P*6(3)22 for a pair of enantiomers with the formula of $[(Ag\mathbf{L^2}_{2/3})_3(Ag\mathbf{L^2})_2](CF_3SO_3)_5$ (Δ-**1** and Λ-**1**), which contains two types of honeycomb metal-organic networks (vide infra). The anion was well-identified by IR spectra, and the phase purity of bulky sample was confirmed by XRD patterns. The thermogravimetric analysis (TGA) performed in air indicated that the crystal tubes were stable up to 300 °C (see the Supporting Information, Figure S1).

Under optical microscopy, it is clear that all visible crystals have 30° staggered hexagonal inner channels. Examination

* Corresponding author. E-mail: cesscy@mail.sysu.edu.cn.

(1) (a) Eisenberg, B. *Acc. Chem. Res.* **1998**, *31*, 117. (b) Gupta, M.; Bagaria, A.; Mishra, A.; Mathur, P.; Basu, A.; Ramakumar, S.; Chauhan, V. S. *Adv. Mater.* **2007**, *19*, 858−861.
(2) Iijima, S. *Nature* **1991**, *354*, 56.
(3) (a) Ajayan, P. M. *Chem. Rev.* **1999**, *99*, 1787. (b) Patzke, G. R.; Krumeich, F.; Nesper, R. *Angew. Chem., Int. Ed.* **2002**, *40*, 2446. (c) Ma, R.; Bando, Y.; Sato, T.; Tang, C.; Xu, F. *J. Am. Chem. Soc.* **2002**, *124*, 10668. (d) Cheng, J.; Guo, R.; Wang, Q.-M. *Appl. Phys. Lett.* **2004**, *85*, 5140. (e) Viculis, L. M.; Mack, J. J.; Kaner, R. B. *Science* **2003**, *299*, 1361. (f) Huang, L.; Wang, Z.; Sun, J.; Miao, L.; Li, Q.; Yan, Y.; Zhao, D. *J. Am. Chem. Soc.* **2000**, *122*, 3530.
(4) (a) Bong, D. T.; Clark, T. D.; Granja, J. R.; Ghadiri, M. R. *Angew. Chem., Int. Ed.* **2001**, *40*, 988. (b) Seo, M.; Seo, G.; Kim, S. Y. *Angew. Chem., Int. Ed.* **2006**, *45*, 6306.
(5) (a) Whitesides, G, M.; Grzybowski, B. *Science* **2002**, *295*, 2418. (b) Ikkala, O.; Brinke, G. *Science* **2002**, *295*, 2407. (c) Lee, H. Y.; Nam, S. R.; Hong, J.-I. *J. Am. Chem. Soc.* **2007**, *129*, 1040. (d) Jeong, J. S.; Lee, J. Y.; Cho, J. H.; Suh, H. J.; Lee, C. J. *Chem. Mater.* **2005**, *17*, 2752.
(6) (a) Uemura, T.; Kitagawa, S. *Chem. Lett.* **2005**, *34*, 132. (b) Raez, J.; Manners, I.; Winnik, M. A. *J. Am. Chem. Soc.* **2002**, *124*, 10381.
(7) (a) Kitagawa, S.; Kitaura, R.; Noro, S.-i. *Angew. Chem., Int. Ed.* **2004**, *43*, 2334. (b) Yaghi, O. M.; O'Keeffe, M.; Ockwig, N. W.; Chae, H. K.; Eddaoudi, M.; Kim, J. *Nature* **2003**, *423*, 705. (c) Leininger, S.; Olenyuk, B.; Stang, P. J. *Chem. Rev.* **2000**, *100*, 853. (d) Li, Y.-H.; Su, C.-Y.; Goforth, A. M.; Shimizu, K. D.; Gray, K. D.; Smith, M. D.; zur Loye, H.-C. *Chem. Commun.* **2003**, 1630.
(8) Uemura, T.; Horike, S.; Kitagawa, S. *Asian J. Chem.* **2006**, *1*−*2*, 36.
(9) (a) Reches, M.; Gazit, E. *Science* **2003**, *300*, 625. (b) Leclair, S.; Baillargeon, P.; Skouta, R.; Gauthier, D.; Zhao, Y.; Dory, Y. L. *Angew. Chem., Int. Ed.* **2004**, *43*, 349.
(10) (a) Su, C.-Y.; Goforth, A. M.; Smith, M. D.; zur Loye, H.-C. *J. Am. Chem. Soc.* **2004**, *126*, 3576. (b) Lu, W.-G.; Su, C.-Y.; Lu, T.-B.; Jiang, L.; Chen, J.-M. *J. Am. Chem. Soc.* **2006**, *128*, 34. (c) Su, C.-Y.; Smith, M. D.; zur Loye, H.-C. *Angew. Chem., Int. Ed.* **2003**, *42*, 4085.
(11) Crystal data: Δ-**1**: $C_{221}H_{192}Ag_5F_{15}N_{24}O_{15}S_5$, $M_r = 4408.64$, hexagonal, space group *P*6(3)22, $a = 17.9391(3)$ Å, $c = 38.4446(13)$ Å, $V = 10714.4(4)$ Å^3, $Z = 2$, $\rho_{calcd} = 1.367$ g cm^{-3}, μ (Cu, Kα) = 4.704 mm^{-1}, $T = 150$ (2) K, 5570 unique reflections out of 30788 with $I > 2\sigma(I)$ ($R_{int} = 0.0464$), final R1 = 0.0678, wR2 = 0.1449. Flack parameter, 0.02(2). Λ-**1**: $C_{221}H_{192}Ag_5F_{15}N_{24}O_{15}S_5$, $M_r = 4408.64$, hexagonal, space group *P*6(3)22, $a = 17.9074(4)$ Å, $c = 38.5402(17)$ Å, $V = 10703.1(6)$ Å^3, $Z = 2$, $\rho_{calcd} = 1.368$ g cm^{-3}, μ (Cu, Kα) = 4.709 mm^{-1}, $T = 150$ (2) K, 5505 unique reflections out of 29583 with $I > 2\sigma(I)$ ($R_{int} = 0.0670$), final R1 = 0.0757, wR2 = 0.1649. Flack parameter, 0.02(2).

10.1021/cm071767u CCC: $37.00
Published on Web 08/21/2007

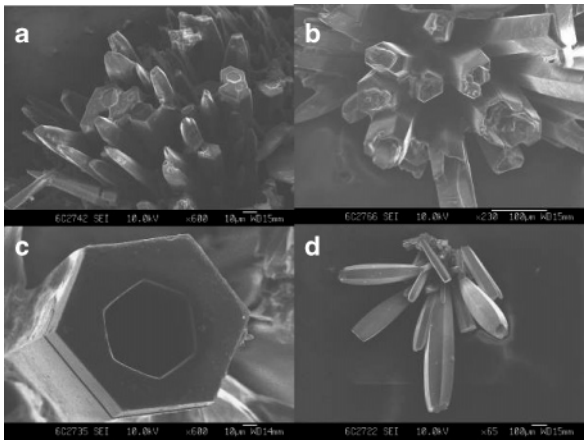

Figure 1. SEM images showing size and shape evolution of tubular crystals: (a) rodlike crystals starting dissolving; (b) partly growing hollow rods; (c) a well-developed tube; and (d) over-grown tubes.

Scheme 1. Ligand Structure and Formation of Two Types of (6,3) Nets

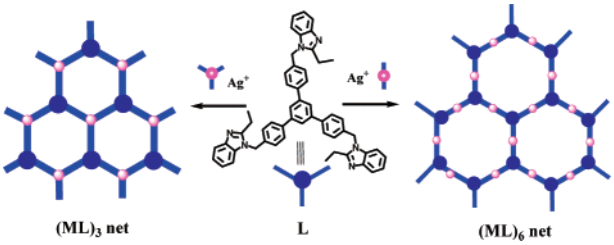

of bulky samples using scanning electronic microscopy (SEM) confirmed that most of the well-grown crystals were in tubular shape. Reproducible growth of crystal tubes indicated that the tubular shape was unique to complex **1** and that the tube size can go down to microscale. Typically, the crystal tubes were grown into a wide range of dimensions with the width in tens to hundreds of micrometers, length in hundreds of micrometers to several millimeters, and thickness in several to tens of micrometer. Besides the tubular crystals, there also exist some small hexagonal rodlike crystals. It is noticeable that many rodlike crystals have incomplete shapes exhibiting various burgeoning hollow appearance. This observation may be informative in understanding the growth procedure of the tubular crystals. Figure 1 shows SEM images taken from a batch of sample, indicative of different tube evolution stages. Within a certain growing period, some small rod crystals are just starting to form holes at the top, some becoming hollow with channels not completely developed, and some have already evolved into well-shaped tubes. It is clear that tubular morphology is not the initial crystal growing shape, therefore, tube shape evolution may undergoes a slow transformation process depending on the growth of the rodlike precursors.

One the basis of SEM observations, the following tube growth steps may be speculated as depicted in Scheme 2: At the beginning, the metal−ligand self-assembly in solution resulted in the formation of coordination networks, which crystallized initially as crystal rods. This is expected, because the crystal is in a hexagonal crystal system and the (001) face is normally the fast growing direction. As more rod crystals formed and the concentration lowered, the growth speed slowed down and the local equilibrium between

Scheme 2. Possible Tube Shape Evolution Steps: (a) Self-Assembly of Coordination Networks in Solution; (b) Initial Crystallization of Rodlike Crystals; (c) Dissolution of Rodlike Precursors Leading to Reassembly of Coordination Network; (d) Recrystallization at Rim of Rod Crystal on (001) Face Leading to Formation of Tube

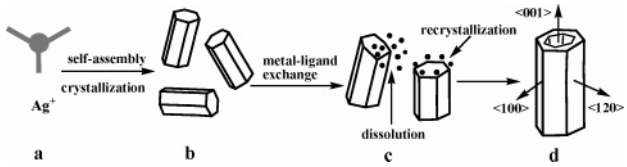

crystallization and dissolution was achieved. This is typical for a coordination self-assembly procedure, which is known to be accomplished via a rapid metal−ligand exchange in solution. At this stage, crystal growth along the preferential direction will dominate easily over other directions. Because the rim of the crystal rod on the (001) face could provide more space for metal−ligand exchange than the face center, recrystallization at the boundary of this face allows more opportunities to take place. Therefore, a slow rod-to-tube transformation occurred as the rod crystals gradually dissolved and the tube wall gradually evolved. Meanwhile, dissolution in the center may cause a shape transition of the resulting channel, as demonstrated in the Supporting Information, Scheme S1. Usually, the fast growth directions are also the fast dissolving directions, therefore, faster dissolution along the <100> directions relative to the <120> directions will finally result in 30° rotation of the inner hexagonal channel. Such a dissolution−recrystallization process may take advantage of reassembly of the coordination network via kinetically reversible metal−ligand exchange, which is different from the often-reported scrolling or template mechanism for inorganic nanotubes.[3] A similar rod-to-tube transformation has been observed for ZnO microtubes, but it underwent a coalescence process at a high temperature.[5d]

Considerable attention is currently paid to fabrication of microtubes[5] because formation of lager inner cavity compared with nanotubes is believed to enable easier modifications of inner surface and imparts more inner platforms to act as containers or reactors for host−guest chemistry or catalytic reactions. In this aspect, microtubes grown from coordination polymers are of interest because of their structural versatility and adjustability.

One structural feature in the present microtube is the appearance of the coexisting network diversity and Borromean topology. The single-crystal structural analysis confirmed that two types of honeycomb networks[12] coexist in the same crystal, as shown in Scheme 2 and panels a and b in Figure 2. In both networks, the ligands display the trimonodentate coordination mode, whereas the Ag^+ ions exhibit two kinds of coordination geometries. One is in triangle connecting three different ligands to form $(\mathbf{ML})_3$ type (6,3) net, and the other is linear to bind two ligands resulting in $(\mathbf{ML})_6$ type (6,3) net. The basic building unit of the $(\mathbf{ML})_3$ net is **AgL**, whereas that of $(\mathbf{ML})_6$ net is $\mathbf{AgL}_{2/3}$, corresponding to metal-to-ligand ratios of 1:1 and 3:2,

(12) (a) Batten, S. R.; Robson, R. *Angew. Chem., Int. Ed.* **1998**, *37*, 1460. (b) Carlucci, L.; Ciani, G.; Proserpio, D. M.; Spadacini, L. *CrystEngComm.* **2004**, *6*, 96.

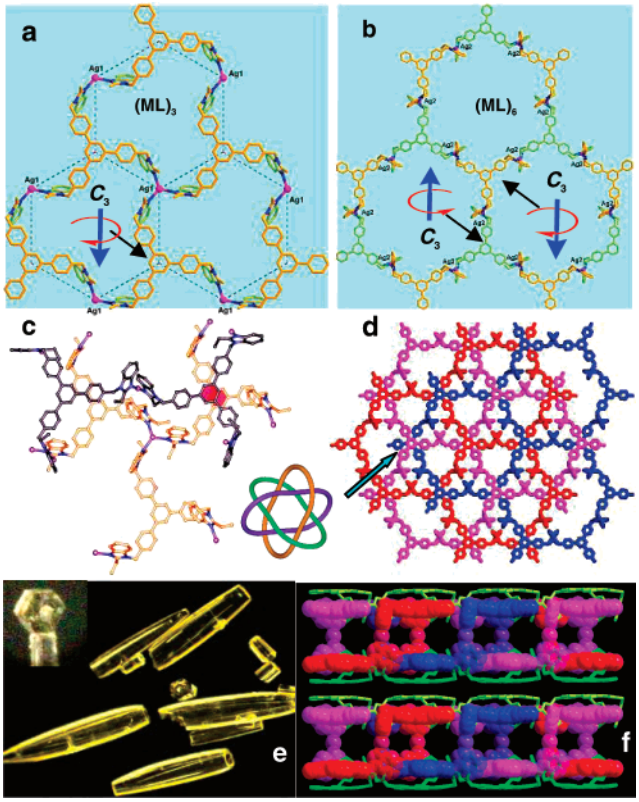

Figure 2. (a) $(\mathbf{ML})_3$ type (6,3) net in Δ-**1** showing right-handed propeller conformation; (b) $(\mathbf{ML})_6$ type (6,3) net in Δ-**1** showing right-handed **AgL** subunits; (c) molecular structures in **1** showing coordination geometry of Ag^+ ions and $\pi\cdots\pi$ stacking (highlighted in red); (d) formation of Borromean layer via 3-fold interlocking of $(\mathbf{ML})_6$ (6,3) nets in Λ-**1** (insert showing Borromean topology); (e) tubular crystals of **1** (insert showing a single-crystal for data collection); (f) parallel stacking of two types of nets resulting in sandwiched Borromean sheets (Borromean layer in space-filling mode).

respectively. Such network diversity in one single crystal remains rare.[12b]

Stacking of the two types of (6,3) networks in the crystal lattice is also unique because of the co-occurrence of both interweaving and non-interweaving polymeric networks in one single crystal. As shown in Figure 2d, the $(\mathbf{ML})_6$ networks are 3-fold interlocked in parallel. However, any two of three entangled nets are free of interlocking, and each individual net lays above another independently. Nevertheless, the existence of the third net causes an inseparable interweaving of three nets, characteristic of Borromean topology, which shows nontrivial three-ring links inseparable as a whole whereas cleavage of any ring makes the whole fall apart.[13] On the contrary, the $(\mathbf{ML})_3$ networks are independent and lay face-to-face on two sides of the Borromean $(\mathbf{ML})_6$ layer via $\pi\cdots\pi$ interactions. Such stacking leads to sandwiched Borromean sheets, as shown in Figure 2f. The counter anions are located between the sheets or inside the Borromean layers, as shown in the Supporting Information, Figure S2.

Another structural feature of the microtube is the chirality of each individual tube. Several tubular crystals as seen in Figure 1e were randomly selected to determine the single-crystal structure, all giving the same chiral space group *P*6(3)22. This indicates that each crystal tube is optically pure. Because there is not any absolute chiral center in the ligand, the individual chiral crystal has to be spontaneously resolved from a racemic mixture containing equivalent enantiomeric tubes. Careful structural analysis did reveal two opposite chiralities, right-handed Δ-**1** and left-handed Λ-**1**, constituting a pair of enantiomers that were confirmed by satisfactory refinement of Flack parameters close to zero.

The chirality of the networks is due to the semirigidity of the tripodal pendant ligand. The ligand itself is achiral because three benzimidazole pendants are free rotatable. Once the ligand displays syn,syn,syn-conformation with three pendants wrapping around the central base in a clockwise or anticlockwise propeller fashion, a C_3 symmetry is imposed, thus endowing intrinsic chirality. This is the case in the two (6,3) networks, as shown in panels a and b in Figure 2 and the Supporting Information, Figure S3. During the network self-assembly, the chiral propeller conformation of ligand is fixed and transferred via the metal−ligand interactions. The $(\mathbf{ML})_3$ network is composed of the same handed **AgL** subunits connected through the C_3-symmetry on Ag^+ ions, whereas the $(\mathbf{ML})_6$ network consists of the same chiral $\mathbf{AgL}_{2/3}$ subunits connected through the C_2-symmetric Ag^+ ions. Therefore, the same absolute conformation propagates within the network and crystal lattice, causing same handedness of the single crystal. If three benzimidazole pendants are arranged around the central C_3 axis in a right-handed way, Δ-enantiomer is produced. On the contrary, left-handed arrangement of pendants will give rise to Λ-enantiomer.

In summary, self-assembly of Ag^+ ions with a tripodal pendant ligand results in two types of honeycomb coordination networks, which cocrystallize to resolve enantiomeric single-crystal tubes showing microscale crystal pores. Some structural features, such as Borromean topology, conformational chirality, and network diversity and entanglement, which are typical for coordination polymers, have been observed in microscale crystal growth. This suggests a possible route for nano/microcrystal growth on the basis of coordination self-assembly. Crystal engineering of coordination polymers with an effort on crystal morphology control, which is essential for nanoscience, may be helpful to introduce various advantages inherent in coordination assemblies into nanomaterials: (a) versatile optic, electronic, or magnetic metal sites; (b) easy molecular modification and network diversification; and (c) embedding structural features of chirality, porosity, topology, and so on.

Acknowledgment. This work was supported by the NSF of China (Grant. 20525310 and 20673147) and 973 Program of China (Grant. 2007CB815302).

Supporting Information Available: Synthesis and characterization, structural solution and refinement, Figures S1−S3 and Scheme S1 (PDF). Crystallograpic information in CIF format. This information is available free of charge via the Internet at http://pubs.acs.org.

CM071767U

(13) (a) Carlucci, L.; Ciani, G.; Proserpio, D. M. *CrystEngComm.* **2003**, *6*, 269, and references therein. (b) Lv, X.-Q.; Pan, M.; He, J.-R.; Cai, Y.-P.; Kang, B.-S.; Su, C.-Y. *CrystEngComm.* **2006**, *8*, 827. (c) Dobrzańska, L.; Raubenheimer, H. G.; Barbour, L. J. *Chem. Commun.* **2005**, 5050. (d) Liantonio, R.; Metrangolo, P.; Meyer, F.; Pilati, T.; Navarrin, W.; Resnati, G. *Chem. Commun.* **2006**, 1819.